Stress tunable magnetoelectric bending resonance for sensing static magnetic field

Xin Zhuang, May-Tia Yang, Marc Lam Chok Sing, Christophe Dolabdjian, Peter Finkel, Jiefang Li, Dwight Viehland

Stress tunable magnetoelectric bending resonance for sensing static magnetic field

X. Zhuang, M. Yang, M. Lam Chok Sing, C. Dolabdjian, P. Finkel, J. Li and D. Viehland

***Abstract*— Magnetostrictive-piezoelectric composite in bi-layer structure shows a resonant enhancement for the mechanical strain mediated magnetoelectric coupling when operating under bending mode. Such composite is of importance to achieve ultrasensitive magnetometers for detecting quasi-static magnetic fields by measuring the parameter variation near the resonant frequency. Detection performance is limited by diverse noise processes appearing in the composite and associated electronics such as the extrinsic interferences due to the environmental vibration and temperature and loss noise sources produced by the energy dissipation in the composite. Since the bending resonance is based on the mechanical interactions in the composite, the noise source due to the thermo-mechanical dissipation becomes an importance noise process to be investigated. In this paper, we investigate the field detection performance relating to the thermo-mechanical and thermo-electric dissipation in a doubly clamped magnetoelectric composite by means of modulation techniques.**

***Index Terms*—Magnetoelectric effects, Equivalent Circuits Modeling, Magnetic field measurement**

I. Introduction

Magnetic field sensing can be achieved by using a magnetoelectric composite consisting of magnetostrictive and piezoelectric phases as a magnetic field sensor. The sensitivity, termed magnetoelectric coefficient could be studied by applying a reference magnetic field and measuring the charge or voltage response through the direct magnetostrictive-piezoelectric effect [1]-[3]. In this case, the ME coefficient is proportional to the product of the piezoelectric and piezomagnetic coefficients, where the latter can be enhanced by a biased magnetic field to reach the maximal sensitivity. Thus, by amplifying the electric output, ones can achieve the passive detection of magnetic fields. By amplifying the electric output, ones can achieve the passive detection of magnetic fields. Under the passive detection mode, noise performances are limited by the dielectric loss in sample or the noise sources in the amplifier.

Besides, other methods based on carrier modulations with the ME composite can be applied for sensing magnetic field by modulating coefficients such as the flexibility, the magnetostriction [4]-[7]. Under an exterior magnetic field, the change of either coefficient can produce an extrinsic parameter change which results to increase or reduce a measureable output due to physical coefficients. For example, a magnetic field induced stress or strain can be measured as a function of the transfer function or the resonant frequency variation. The working method can be classified into magnetic and electric excitation according to the excitation types. The former depends on an oscillating magnetic field producing a magnetostrictive strain on the composite by using an excitation coil. High energy consumption is required because of the current in the excitation coil. The latter employs an excitation voltage across the piezoelectric layer to generate a strain or stress on the composite through the piezoelectric effect.

An analytic method is based on the equivalent circuit of a magnetoelectric composite which could be regarded as a system with several elements exhibiting magnetic, electric and mechanical properties. The sensitivity to a magnetic field can be calculated with the help of this circuit. Besides, the energy dissipations can be integrated into these elements by considering the noise theory in an electric system. Thus, fluctuations due to the energy dissipation lead to, in detection process, an incertitude which is generally referred to as amplitude noise or phase noise at the output side. The electric and mechanical energy losses dominate the main noise sources in a ME. The electric dissipation produces incertitude on the electric capacitance as electric loss noise source. And the mechanical noise sources are due to the dissipation in elastic elements such as the mechanical capacitance or the resistance.

II. Electric excitation method on ME composite

A. Spring-mass-damper modeling

A magnetostrictive-piezoelectric bi-layer composite can be modulated by two transducers. In general, a traditional equivalent circuit modeling can be created by using the constitutive equations with the flexibility, piezoelectric coefficients, etc. However, theses coefficients are not always perfectly fit to the measurement in practice due to diverse

Manuscript received October 9, 2001. (Write the date on which you submitted your paper for review.) This work was supported in part by the U.S. Department of Commerce under Grant BS123456 (sponsor and financial support acknowledgment goes here).

X. Zhuang, M. Yang, M. Lam Chok Sing and C. Dolabdjian are with the Normandy Univ, France; UCBN, GREYC, F-14032 Caen, France; CNRS, UMR 6072, F-14032 Caen, France (e-mail: xin.zhuang@unicaen.fr, may-tia.yang@ensicaen.fr, marc.lam@ensicaen.fr, christophe.dolabdjian@unicaen.fr).

P. Finkel is with the U.S. Naval Research Laboratory, Washington, D.C. 20375, USA (e-mail: peter.finkel@navy.mil).

J. LI and D. Viehland are with the Materials Science and Engineering, Virginia Tech., Blacksburg, VA 24061, USA (e-mail: jiefang@mse.vt.edu, viehland@mse.vt.edu).

factors such as the imperfect bonding between layers, demagnetization and/or excitation in a ME composite. This produces an enormous error between the approaching result and the one in practice [8]-[10]. However, a driven-damped calculation based on the spring-mass-damper modeling, which is simplified from the equivalent circuit, can serve to simulate the sensitivity and noise by measuring the mechanical and electric parameters in the circuit. The inertia, elastic and damping terms can be defined as three mechanical parameters: the mechanical inductance L_m, the mechanical capacitance C_m and the mechanical resistance R_m, respectively. Besides, the piezoelectric coupling is defined by a parameter φ_p. By using the equivalent circuit modeling [11], the equivalent sensor capacitance, C_{sensor}, can be developed from Fig. 1. C_0 is the constant part of the electric capacitance which is invariant from the mechanical parameters or the piezoelectric coupling parameter. C_{PE} is the capacitance contribution from the piezoelectric effect. The mechanical impedance consisting of L_m, C_m and R_m is defined as Z_m. Thus, the expression of the sensor capacitance is presented as

$$\begin{aligned} C_{sensor} &= C_0 + C_{PE} \\ &= C_0 + \frac{\varphi_p^2}{j\omega\left(R_m + j\omega L_m + \frac{1}{j\omega C_m}\right)}, \end{aligned} \tag{1}$$

where ω is the angular frequency of the applied signal.

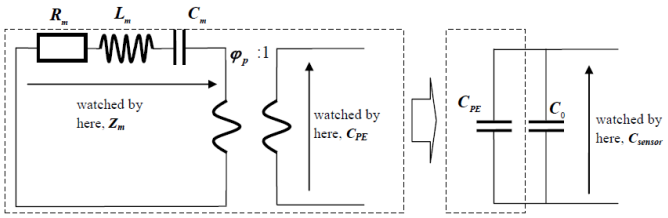

Fig. 1: Equivalent circuit model of a ME laminated sensor.

For a mechanical detection such as the phase or amplitude measurement around the resonant frequency, the mechanical quality is an important factor for the sensor performance [12], [13]. This factor Q_m, is given as

$$Q_m = \frac{1}{R_m}\sqrt{\frac{L_m}{C_m}} \tag{2}$$

By taking into count the transformed expression of the mechanical quality, $Q_m = \frac{\omega_{res} L_m}{R_m} = \frac{1}{\omega_{res} C_m R_m}$ where ω_{res} is the angular resonant frequency. The mechanical impedance can be rewritten as a function of the mechanical resistance, the mechanical quality and a dissonant factor δ_{diss} [14].

$$\begin{aligned} Z_m &= R_m + j\omega L_m + \frac{1}{j\omega C_m} \\ &= R_m\left(1 + jQ_m\delta_{diss}\right) \end{aligned} \tag{3}$$

where, $\delta_{diss} = \frac{\omega}{\omega_{res}} - \frac{\omega_{res}}{\omega} = \frac{2\Delta f}{f_{res}}$, $\Delta f = \frac{\omega - \omega_{res}}{2\pi}$ and $f_{res} = \frac{\omega_{res}}{2\pi}$.

Δf is defined as a small frequency shift between the excitation frequency and the resonant one.

In order to sense low frequency magnetic fields, the time or frequency dependent parameter can be measured. The time depending parameters consists of the amplitude and phase of the voltage. A low frequency magnetic field can modulate these time-variant parameters to achieve the magnetic field sensing by using a modulation-demodulation process. However, frequency dependent parameters, such as the resonant frequency, can also be used to detect static or quasi-static magnetic field.

A composite under asymmetric structure can produce a bending resonant frequency in low frequencies [15], [16]. Around this frequency, the voltage-charge transfer function is much more sensitive to an external force than the ones far from the resonant frequency. The response of the transfer function to the stress induced change of the sensor capacitance reaches its maximum value. The real part and imaginary part of the sensor capacitance can be derived with the help of (1). Thus, the electric transfer function with a charge amplifier [17] can be written as

$$\begin{aligned} Tr_{EE} &= 1 + \frac{C_0}{C_1} + \frac{\varphi_p^2}{C_1\left(j\omega R_m + \frac{1}{C_m} - \omega^2 L_m\right)} \\ &= 1 + \frac{C_0}{C_1} + \frac{\varphi_p^2}{\omega C_1 |Z_m|^2}\left(\frac{1}{\omega C_m} - \omega L_m\right) - j\frac{\varphi_p^2 R_m}{\omega C_1 |Z_m|^2} \\ &= \mathrm{Re}(C_m) + j\,\mathrm{Im}(C_m) \end{aligned} \tag{4}$$

where C_1 is the feedback capacitance in the charge amplifier and $\mathrm{Re}(C_m)$ and $\mathrm{Im}(C_m)$ are the real and imaginary part of the transfer function, with

$$\begin{cases} \mathrm{Re}(C_m) = 1 + \frac{C_0}{C_1} + \frac{\varphi_p^2}{\omega C_1 |Z_m|^2}\left(\frac{1}{\omega C_m} - \omega L_m\right) \\ \mathrm{Im}(C_m) = -\frac{\varphi_p^2 R_m}{\omega C_1 |Z_m|^2} \end{cases}$$

Thus, the gain and the phase response to an exterior magnetic field are given by

$$\begin{cases} \frac{\partial |T_{rEE}|}{\partial H} = \frac{1}{|T_{rEE}|}\left(\mathrm{Re}(C_m) \times \frac{\partial \mathrm{Re}(C_m)}{\partial H} + \mathrm{Im}(C_m) \times \frac{\partial \mathrm{Im}(C_m)}{\partial H}\right) \\ \frac{\partial \psi}{\partial H} = \frac{1}{|T_{rEE}|^2}\left(\mathrm{Re}(C_m) \times \frac{\partial \mathrm{Im}(C_m)}{\partial H} - \mathrm{Im}(C_m) \times \frac{\partial \mathrm{Re}(C_m)}{\partial H}\right) \end{cases} \tag{5}$$

With the gain $|T_{rEE}| = \sqrt{\mathrm{Re}(C_m)^2 + \mathrm{Im}(C_m)^2}$ and the phase $\psi = \arctan[\frac{\mathrm{Im}(C_m)}{\mathrm{Re}(C_m)}]$

By inserting the expressions of the real and imaginary parts into (5), it yields

$$\frac{\partial|T_{rEE}|}{\partial H}=\frac{1}{|T_{rEE}|}\times\left[\left(1+\frac{C_0}{C_1}-\frac{\varphi_p^2}{C_1}\times\frac{A}{\omega|Z_m|^2}\right)\left(-\frac{\varphi_p^2}{\omega^2C_1C_m^2|Z_m|^2}\right)\left(1-\frac{2A^2}{|Z_m|^2}\right)-\left(\frac{\varphi_p^2R_m}{C_1\omega|Z_m|^2}\right)\left(\frac{2\varphi_p^2R_mA}{\omega C_1C_m^2|Z_m|^4}\right)\right]\times\frac{\partial C_m}{\partial H} \tag{6}$$

where $A=\omega L_m-\frac{1}{\omega C_m}$ is the mechanical reactance.

The resonant amplitude is sensitive to the field tuned mechanical capacitance. This is caused by the flexure flexibility of the sensor which changes as a function of the field-induced force. Similarly, the real and imaginary response to a low frequency magnetic field can result a phase shift of the transfer function. This phase response to an external magnetic field becomes,

$$\frac{\partial\psi}{\partial H}=\frac{1}{|T_{rEE}|^2}\times\left[\frac{2\varphi_p^2R_mA}{\omega C_1C_m^2|Z_m|^4}\left(1+\frac{C_0}{C_1}-\frac{\varphi_p^2A}{\omega C_1|Z_m|^2}\right)-\frac{\varphi_p^4R_m}{\omega^3C_1^2C_m^2|Z_m|^4}\left(1-\frac{2A^2}{|Z_m|^2}\right)\right]\times\frac{\partial C_m}{\partial H} \tag{7}$$

Particularly, at the mechanical bending resonant angular frequency, ω_{res}, we have $A=0$. This simplifier the above formula into,

$$\frac{\partial|T_{rEE}|}{\partial H}=\frac{-1}{|T_{rEE\_res}|}\left(1+\frac{C_0}{C_1}\right)\frac{S_{\max}Q_m}{C_m}\times\frac{\partial C_m}{\partial H} \tag{8}$$

where $S_{\max}=\frac{\varphi_p^2}{\omega_{res}C_1R_m}$ is the maximum absolute value of the imaginary part, $|T_{rEE\_res}|$ is the absolute value of the transfer function at the bending resonant frequency.

$$\frac{\partial\psi}{\partial H}=\frac{1}{|T_{rEE\_res}|^2}\times\frac{S_{\max}^2Q_m}{C_m}\times\frac{\partial C_m}{\partial H} \tag{9}$$

If w define $Cos\theta=\frac{1+C_0/C_1}{|T_{rEE\_res}|}$, $Sin\theta=\frac{S_{\max}}{|T_{rEE\_res}|}$, (8) and (9) become

$$\begin{cases}\frac{\partial|T_{rEE}|}{\partial H}=-\left(1+\frac{C_0}{C_1}\right)\frac{Q_m\sin\theta}{C_m}\times\frac{\partial C_m}{\partial H}\\ \frac{\partial\psi}{\partial H}=\frac{Q_m\sin^2\theta}{C_m}\times\frac{\partial C_m}{\partial H}\end{cases}, \tag{10}$$

where θ is defined as an electro-elastic angular which presents the ratio between the capacitance produced by the mechanical and dielectric effect.

Sensors based on the piezomagnetic or piezoelectric resonances have been theoretically and experimentally investigated for sensing strain stress or small mass by changing the flexibility of the sensor [18], [19]. A magnetic field induced resonant frequency shift defines the sensitivity of the resonant frequency to an exterior magnetic field. By measuring this resonant frequency shift, low frequency magnetic fields can be reconfigured [20]. The sensitivity has the form

$$\frac{\partial\omega_{res}}{\partial H}=-\frac{\omega_{res}}{2C_m}\frac{\partial C_m}{\partial H} \quad . \tag{11}$$

The resonant frequency defined in this paper is the frequency which can maximize the mechanical response of the ME composite. The resonant frequency shift is produced by the magnetostrictive-stress-induced flexibility change, which is related to the mechanical capacitance C_m. So the sensitivity can be developed in the formula $\frac{\partial\omega_{res}}{\partial H}=\frac{\partial\omega_{res}}{\partial C_m}\times\frac{\partial C_m}{\partial F}\times\frac{\partial F}{\partial H}$.

The maximum value of imaginary part of the electric transfer function is another parameter depending on the exterior magnetic field. The analytical expression can be developed as a function of $\frac{\partial C_m}{\partial H}$. By applying a small magnetic field, we suppose that $\frac{\partial C_m}{\partial H}$ is the dominant term in the sensing process. Thus, we have

$$\frac{\partial S_{\max}}{\partial H}=\frac{S_{\max}}{2C_m}\times\frac{\partial C_m}{\partial H}, \tag{12}$$

Similarly to the detection on the resonant frequency, the sensitivity by detecting the maximal absolute value can be developed in the formula $\frac{\partial S_{\max}}{\partial H}=\frac{\partial S_{\max}}{\partial C_m}\times\frac{\partial C_m}{\partial F}\times\frac{\partial F}{\partial H}$.

B. Dissipation

The intrinsic dissipations in a ME composite can be generally classified into three types: magnetic, electric and mechanical energy losses [21]-[23]. Each energy loss can be calculated from the dissipated and stored energy on the area of its hysteric circle [24], [25]. And the three types of energy loss are partially correlated to each other two by two in a ME composite. The dielectric dissipation, relating to the electric energy loss between an electric field and a polarization, determines the intrinsic noise performance in low frequency for passive mode detection. The noise due to the magnetic energy dissipation is a classical noise source with notable influence to the detection with a pick-up coil, where it appears as a main intrinsic noise source. However, only the correlated part of the magnetic dissipation which is transferred into the electric one by mechanical media can contribute to the output noise level for the electric detection. Thus, the magnetic dissipation in a ME composite is nearly negligible comparing to the electric one for an electric detection.

The piezoelectric layer, PMN-PT used in the sensor, is a typical ferroelectric relaxor material [26], [27], where the dielectric dispersion processes can be produced by the kinetics from different defect phenomenon such as the domain wall discontinuous motions and boundary imperfections. Thus, fluctuations can be generated in these dissipative processes. However, the nature of low frequency electric fluctuations is not clearly understood so far, in spite that numerous experimental

results and assumptions have been made. We can assume that the low frequency disordering is related to polarization fluctuation which is not the unique contribution to the low frequency electric noise. There exist other contributions to the low frequency fluctuation such as the temperature fluctuation and the resistivity one. However, the relaxation time due to the defections with domain wall motions and boundaries usually exceeds by magnitudes the one from free electron motions or temperature relaxation time. Thus, the low frequency dissipation due to the fluctuation polarization can become the origin of a dominant noise process. The power spectrum of the electric fluctuation due to the dielectric loss can be derived by using a dielectric loss tangent $\tan(\delta_{elec})$ with the help of the Nyquist's formula. It yields,

$$i_{n\_C_0}^2 = 4k_B T\omega C_0 \tan\left(\delta_{elec}\right) \tag{13}$$

Fluctuations due to the mechanical energy dissipation can also lower the detection performance of a sensor [28], [29]. This energy dissipation is induced by the inter-friction loss and the elastic loss in layers and inter-layers of a ME sensor. As a result of the mechanical fluctuations, the oscillatory amplitude and frequency become uncertain. This dissipation can be regarded as a loss process in the mechanical resistance and capacitance. A force noise source can be partially related to the mechanical inter-friction which determinates the value of the mechanical resistance. By applying the Nyquist's formula, a mechanical fluctuation source can be quantitatively obtained. It yields

$$f_{n\_Z_m}^2 = 4k_B T R_m + 4k_B T \frac{\tan\left(\delta_m\right)}{\omega C_m}, \tag{14}$$

with two dissipative terms R_m and $\tan\left(\delta_m\right)/\omega C_m$. They are both given in accordance with the mechanical resistive and capacitive loss, respectively. k_B is the Boltzmann constant. $\tan(\delta_m)$ is a loss tangent of the flexibility representing the dissipative level in the mechanical capacitance. T is the ambient temperature in Kelvin.

III. Noise Sources

According to the transmission mechanism, the noise source can be generally classified into two types: the passive noise and the modulation noise. The first process occurs without any additional driven signal. However, the latter is a parasitic phenomenon depending on an excitation signal, and usually accompanying with a frequency up-conversion. In this case, the low frequency dissipation distributes as fluctuations around an excitation frequency.

a) Passive noise sources

In order to analyze the noise strength due to the passive contribution from the fluctuation in a ME sensor, we can add a force generator at the mechanical dissipation elements in the equivalent circuit. Thus, the noise transfer function, T_{r_QF}, between a force fluctuation and an output electric charge can be defined as the ratio between a generated charge, ΔQ, and a applied force, ΔF. This can be deduced from the equivalent circuit model in Fig. 1, and it yields

$$Tr_{\_QF} = \frac{\Delta Q}{\Delta F} = \left|\frac{\varphi_p}{\omega Z_m}\right| \tag{15}$$

Thus, with the help of the force transfer function, the passive additive charge noise source, q_{n_Zm}, can be presented as a function of the mechanical force fluctuation. It yields

$$q_{n\_Z_m} = \left|\frac{\varphi_p}{\omega Z_m}\right| f_{n\_Z_m}. \tag{16}$$

The pure electric dissipation due to the electric permittivity loss in the static capacitance C_0 contributes to the output charge noise of a ME sensor. It yields

$$q_{n\_C_0} = \sqrt{4k_B T \tan\delta_{elec} C_0 / \omega} \tag{17}$$

b) Active noise sources under modulation

Active noise sources exhibit as a product of the fluctuation and a carrier in a modulation process [30]. This result a near carrier noise spectral densities in frequency domain. Fluctuation of the resonant frequency and the maximum amplitude at this frequency are two noise sources which must be considered for magnetic field detection by measuring the variation of these two values. The resonant frequency noise spectral density can be given as a function of the mechanical force fluctuation. It yields

$$\omega_{res\_n} = -\frac{\omega_{res}}{2C_m}\frac{\partial C_m}{\partial F} f_n, \tag{18}$$

where $\frac{\partial C_m}{\partial F}$ is the mechanical capacitance variation to an external force. The resonant frequency noise spectral density is directly related to the value of the resonant frequency, the mechanical capacitance, the sensitivity of the mechanical capacitance to an exterior force and the force noise. Thus, the resonant frequency noise depends on an initial value of the mechanical capacitance. This initial value can be fixed by an exterior magnetic bias and/or an exterior force to achieve a tunable resonant frequency.

The mechanical force can also lead to a fluctuation on the maximum absolute amplitude of the imaginary transfer function, which is defined as a noise source for the maximum absolute value. It yields

$$S_{\max\_n} = \frac{S_{\max}}{2C_m}\frac{\partial C_m}{\partial F} f_n \tag{19}$$

This expression consists of a term which depends on the force induced mechanical capacitance change. The mechanical resistance can be also influenced by a mechanical force as well. But the value is nearly constant for fluctuations with small amplitude.

By using amplitude modulation method, the near carrier active noise due to the mechanical dissipation can be expressed as

$$q_{n\_Z_m\_\mathrm{mod}} = \frac{\partial |T_{rEE}|}{\partial C_m} \times \frac{\partial C_m}{\partial F} f_n \tag{20}$$

This is the charge noise source around an excitation signal due to the low frequency mechanical dissipation. Thus, the total output charge noise source is a quadratic sum of (16), (17) and (20). It yields the total charge noise source at the output of the sensor for an amplitude modulation,

$$\begin{aligned} q_n^2 &= q_{n\_Z_m}^2 + q_{n\_Z_m\_\mathrm{mod}}^2 + q_{n\_C_0}^2 \\ &= \left| \frac{\varphi_p}{\omega Z_m} \right|^2 f_n^2 + \left(\frac{\partial |T_{rEE}|}{\partial C_m} \times \frac{\partial C_m}{\partial F} \right)^2 f_n^2 + \frac{2k_B T \tan\delta_{elec} C_0}{\pi f} \end{aligned} \tag{21}$$

In our previous papers [6], we have investigated the noise performance by using the amplitude modulation at the symmetric resonant frequency, where the dominant noise source is the low frequency noise source distributing around the excitation frequency. The noise contribution from the passive mode is lower than the modulation one on the carrier around the mechanical resonant frequency. However, when we drive the sensor by using a lower excitation frequency towards several hundred hertz the passive noise sources presents as the main noise contribution in the detection.

IV. Experimental

A ME composite consisting of a magnetostrictive layer, a piezoelectric layer was fabricated as a magnetic field sensor for low frequency field sensing, shown in Fig. 2 (a). The magnetostrictive layer is made of three foils of Metglas in dimension of xxx. A DC magnetic bias is applied by two magnets in order to achieve a maximal magnetostriction for a AC magnetic field. Five piezoelectric macro-fibers create the piezoelectric layer with a dimension of xxx, bonding to Kapton layers with interdigital electrodes on both the top and bottom surface. Thus, an output voltage U_0 (or a output charge) can be measured through the electrodes across the piezoelectric layer. The working method under the bending mode is given in the Fig. 2 (b). A doubly clamped ME composite is magnetically biased by a pair of magnets along its length direction. A low frequency magnetic field is generated by a Helmholtz coil (not shown in the figure) along the in-plane direction of the sensor. A voltage excitation is applied across the interdigital electrodes to induce a flexure displacement Δu along the out-of-plane direction.

In order to achieve the experimental measurement, the ME sensor is connected to the charge amplifier where the induced charge can be picked up with the help of two pairs of inter-digital electrodes which are disposed on both the top and bottom surfaces of the piezoelectric layer. In order to apply the excitation carrier, a sinusoidal wave generator was connected onto the positive input of the charge amplifier as shown in Fig. 3. A low-frequency magnetic field H, serving as a reference signal, produces a stress on the ME laminate. By injecting a noise input and measuring the response of this noise, the transfer function of this system can be measured as a function of frequencies around the bending resonant frequency.

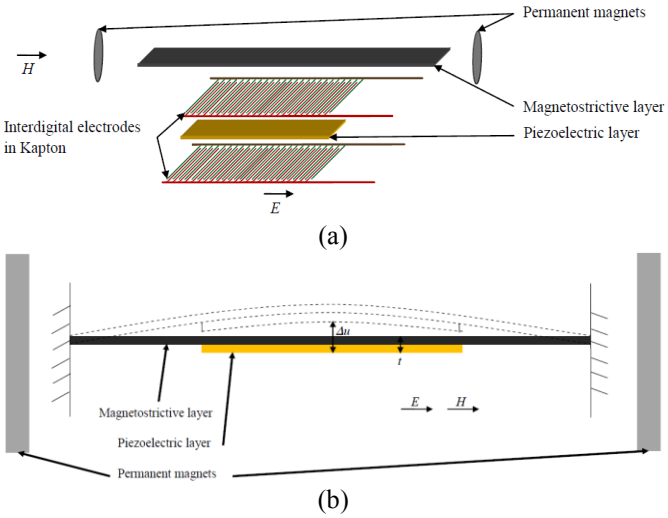

Fig. 2: (a) ME sensor with interdigital electrodes and (b) Sketched figure on the working mode under doubly clamped condition

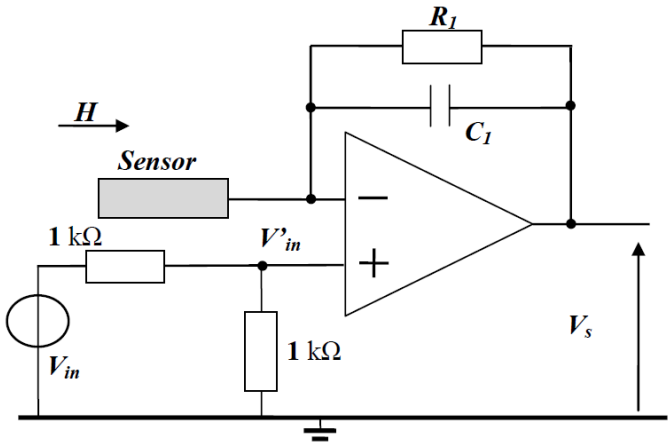

Fig. 3: ME sensor with an associated charge amplifier.

Thus, the electric transfer function, T_{r_EE} in unit [V/V] can be given by the following formula,

$$T_{r\_EE} = \frac{V_S}{V_{in}'} = 2\frac{V_S}{V_{in}} = 2T_{r\_EE}^{mes} \tag{22}$$

where $T_{r\_EE}^{mes} = \frac{V_s}{V_{in}}$ is the measured system transfer function. The measured electric transfer function is shown in Fig. 4.

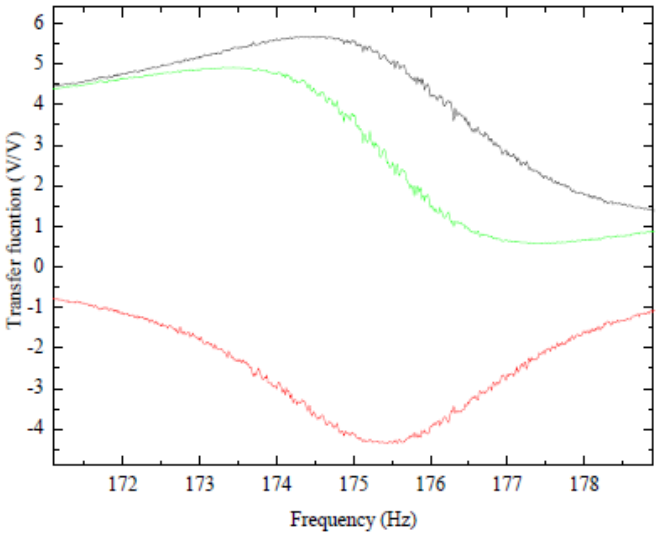

Fig. 4: Real part, imaginary part and gain of the electric transfer function in green, red and black, respectively, as a function of the frequency

In practical, the noise performance can be characterized by two steps. Firstly, the mechanical elements in the equations were obtained or calculated by measuring the electric transfer function around the bending resonant frequency. The mechanical capacitance was obtained from the measured bending resonant frequency ω_{res} at the minimal value on the red curve in Fig. 4 and the dynamic mass L_m of the sensor. Then, the pure electric capacitance can be derived by measuring the maximal and minimal value of the real part of the transfer function, with the help the equation

$$C_0 = \left(\frac{Max\left(\mathrm{Re}\left\{2T_{r\_EE}^{mes}\right\}\right) + Min\left(\mathrm{Re}\left\{2T_{r\_EE}^{mes}\right\}\right)}{2} - 1 \right) C_1 \qquad (23)$$

where $Max\left(\mathrm{Re}\left\{2T_{r\_EE}^{mes}\right\}\right)$ and $Min\left(\mathrm{Re}\left\{2T_{r\_EE}^{mes}\right\}\right)$ are the maximum and minimum of the real part of the electric transfer function. The mechanical quality can be obtained by measuring the tangent value of the transfer function around the bending resonant frequency. It yields

$$Q_m = \frac{1}{\delta_{diss}} \sqrt{\left(\frac{\left(2T_{r\_EE}^{mes}\left(j\omega_{res}\right) - 1\right)C_1 - C_0}{\left(2T_{r\_EE}^{mes}\left(j\omega_{\_\Delta f}\right) - 1\right)C_1 - C_0} \right)^2 - 1} \qquad (24)$$

where $\omega_{\_\Delta f}$ is an angular frequency with a small shift of Δf far from the resonant frequency.

By tuning Δf, the mechanical quality can be characterized as a function of the frequency step number. The step of a frequency shift is 0.0125 Hz in the calculation. By taking a small step number, the measured mechanical quality is inaccurate because noise disturbs the measurement of the transfer function. The obtained mechanical qualities Q_m are around 43 and 56 at 1 Hz (with 80 steps) far from the resonant frequency for the case with and without external magnets, respectively shown in Fig. 5(a). With the help of the measured mechanical qualities, the mechanical resistance R_m is fund as value of either 0.274 or 0.355 [kg/s] for the cases of with or without exterior magnets, respectively, shown in Fig. 5(b).

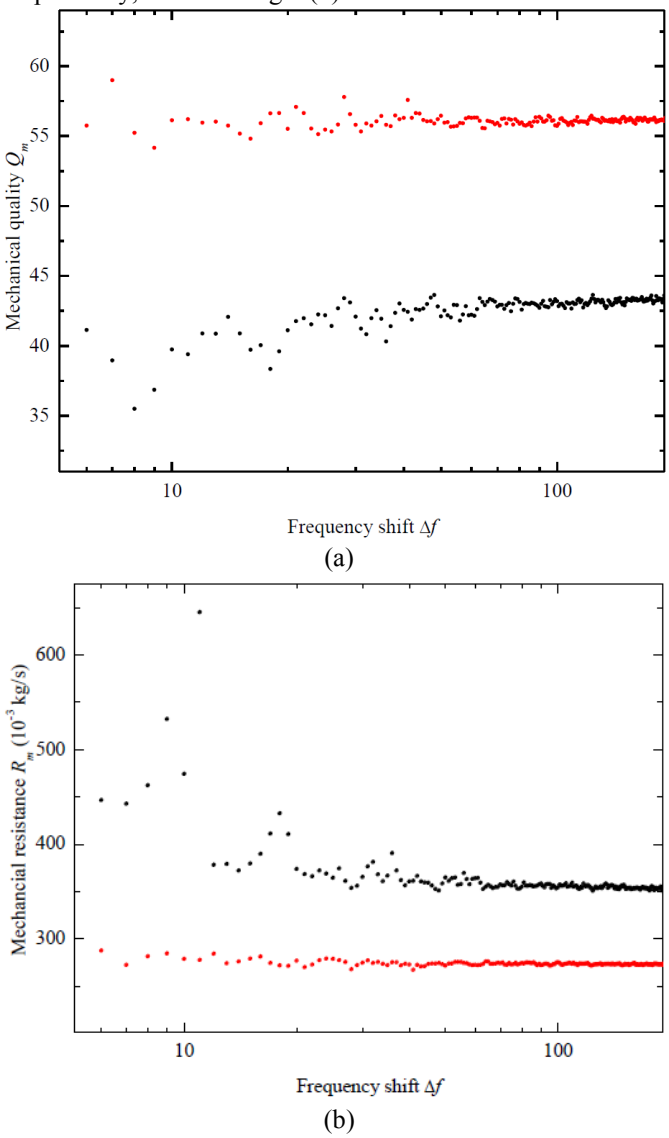

Fig. 5: (a) Mechanical quality and (b) mechanical resistance as functions of the frequency shift step with (red curve) and without (black curve) exterior bias magnets.

Besides of the first bending resonance, the other resonances depending on vibration methods can also be characterized by measuring the electric transfer function. Thus, the imaginary part of the wide bandwidth transfer function can be given in Fig. 6. Resonant peaks based on several vibration modes were observed on the curve of the electric transfer function at resonant frequencies around 175 Hz, 900 Hz and 5500 Hz. In practice, the inter-friction loss in a ME sensor can be assumed as a sum of the velocity dissipation in several vibration modes. By using a similar method in the previous discussion, we can obtain the mechanical quality and the mechanical resistance for each resonant frequency. The inter-friction occurs along the in-plane

direction of the laminate in spite of different vibration modes along the out-of-plane direction. The total force noise spectral power is the quadratic sum of individual ones, which can be calculated from several resonant peaks. Thus the value of the mechanical resistance can be expressed by

$$R_{m\_total} = \sum_n R_{m\_n} \tag{25}$$

where R_{m_n} is the mechanical resistance related to the n^{th} resonant frequency. In the following simulations, we took the first two highest resonant peaks for the calculations, at 175Hz and 5500 Hz.

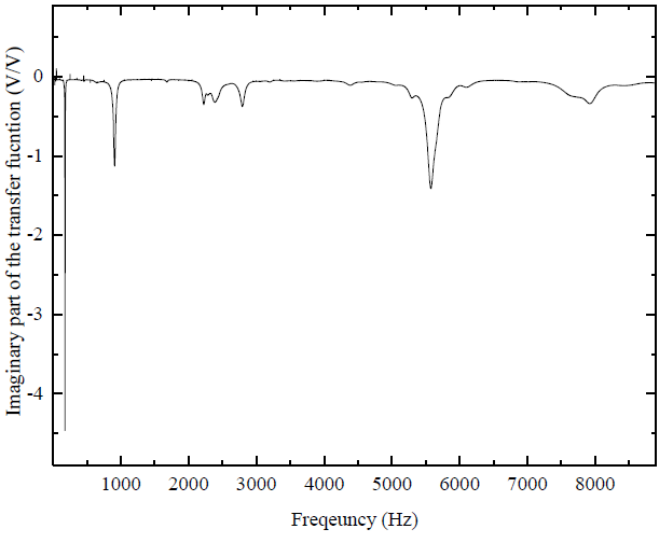

Fig. 6: Imaginary part of the wide bandwidth transfer function as a function of the frequency.

At last, we deduce the piezoelectric coupling coefficient φ_p. This coefficient can be calculated from the value of the transfer function at the bending resonant frequency. It yields

$$\varphi_p^2 = C_1 \omega_{res} R_m S_{\max} \tag{26}$$

With the help of the measured parameters, we can simulate the output voltage noise spectral densities in passive mode. From (24), the output voltage noise at the output of the charge amplifier can be calculated by $e_n = \frac{q_n}{C_1}$. We compare the measured and predicted curves in Fig. 7(a) as well as a zooming-in visualization around the bending resonant frequency, shown in Fig. 7(b). The dashed lines are the simulations curves of the output voltage noise spectral density by using the measured mechanical parameters in passive mode characterization. The output noise spectral density is amplified by the transfer function near mechanical resonant frequency.

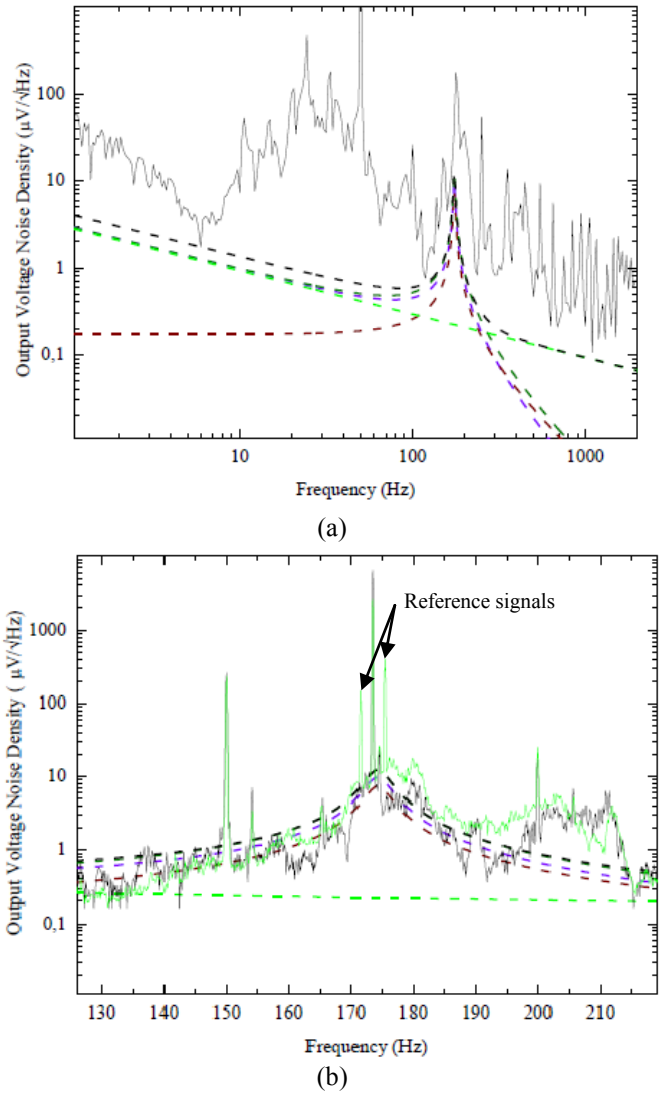

Fig. 7: The noise spectral densities for the (a) wide and (b) on-resonance bandwidth. The dashed lines are the simulation curves for the dielectric loss dissipation in green, the resistive one in dark red, the capacitive one in purple and the total noise spectral density simulation in black. The solid black curves in both (a) and (b) are the measured ones for the passive mode without any reference signal. And the solid green curve is the one with reference signals at 2 Hz.

The force noise can be derived from its theoretical formula by using the value of the mechanical resistance. By using the resistive part of the mechanical force $f_n = \sqrt{4k_B T R_{m\_total}}$ the passive noise spectral density is noise source for the low frequency modulation. In this case, the equivalent magnetic noise spectral density is defined by

$$b_n = \frac{e_n}{T_{r\_ME/EE}} = \frac{\varphi_p}{C_1 \left|\omega Z_{mech}\right| T_{r\_ME\_E/E}} f_n \tag{27}$$

where the magnetic transfer function $T_{r\_ME/EE}$ was measured as a function of the frequency by applying a sinusoidal sweeping signal. By this measuring, we have $T_{r\_ME\_E/E} = \frac{\partial \left|T_{r\_EE}\right|}{\partial H} \times V_{exc} = 158$ [V/T], regarded at the output of

the charge amplifier, for a measurement bandwidth towards 26 Hz which is set as the cutoff frequency of the low-pass filter during the demodulation process.

TABLE I
PARAMETERS FOR SIMULATION

Symbol	Quantity	Value
C_0	Pure electric capacitance	540×10^{-12} F
Lm	Mechanical inductance	14×10^{-3} kg
Cm	Mechanical capacitance	59.5×10^{-6} s^2/kg
Rm	Mechanical resistance	356×10^{-3} kg/s
R_{m_total}	Total mechanical inductance	9 kg/s
φ_p	Piezoelastic factor	7.5×10^{-4} N/V
k_B	Boltzmann constant	1.38×10^{-23}
T	Temperature	300 K
S_{max}	Maximum absolute value of the imaginary part of the transfer function	5.2
ω_{res}	Angular resonant frequency	1087 rad
$tan(\delta e_{lec})$	Dielectric loss factor	0.06
$tan(\delta_m)$	Mechanical loss factor	*0.02
$T_{r\_ME\_E/E}$		**158 V/T

*The mechanical loss is up-limit fitting value.
**This value is related to a normalized transfer function at the output of the charge amplifier where the noise is simulated.

Experimentally, the amplitude modulation has been achieved by using an electric excitation with a frequency near the bending resonant frequency of the composite. Meanwhile, a low frequency magnetic signal was applied in the longitudinal direction as a reference signal. By taking the values of the parameters in above sections, we give the simulation curves as well of the spectral densities as well as the measured one for the equivalent magnetic noise in Fig. 8.

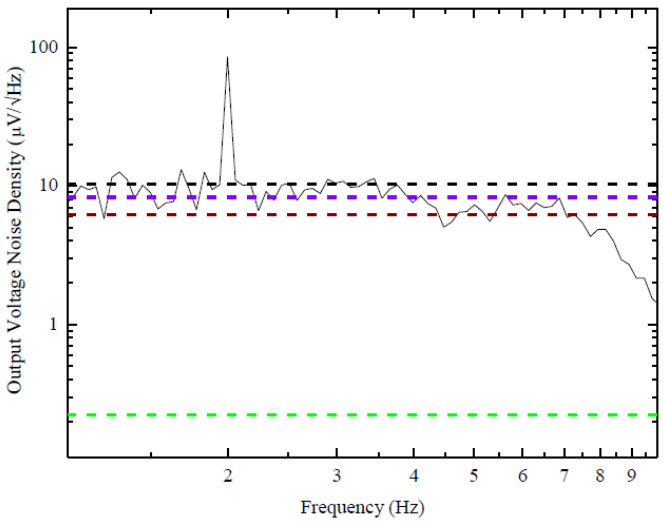

Fig. 8: Equivalent input magnetic noise spectral density as a function of the frequency by using amplitude modulation. The black solid curve is the measured noise spectral density. The dashed green, dark red, purple and black lines are the simulation curves for the dielectric, resistive, capacitive loss and the total one.

V. CONCLUSION

Modulation techniques can be achieved on a magnetostrictive-piezoelectric composite by measuring the variation of the gain, phase, resonant frequency or the maximum peak value under an exterior magnetic field. Fluctuation due to the mechanical dissipation results diverse noise sources for each detection method. A model based on simplified Mason modeling is used to predict the noise performance of a ME sensor for sensing low frequency magnetic field, where the electric and mechanical elements can be characterized by measuring the electric transfer function as a function of frequency around the bending resonant frequency. The experimental curves are in good agreement with the predicted noise performance.

REFERENCES

[1] C. Nan, M. I. Bichurin, S. Dong, D. Viehland and G. Srinivasan, "Multiferroic magnetoelectric composites Historical perspective, status, and future directions," *J. Appl. Phys.,* vol. 103, p. 031101, 2008.

[2] S. Priya, R. Islam, S. Dong and D. Viehland, "Recent advancements in magnetoelectric particulate and laminate composites," *J. Electroceram,* vol. 19, pp. 147-164, 2007.

[3] G. Lawes and G. Srinivasan, "Introduction to magnetoelectric coupling and multiferroic films," *J. Phys. D: Appl. Phys.,* vol. 44, p. 243001, 2011.

[4] H. B. Wang and Z. H. Feng, "A highly sensitivity magnetometer based on the Villari effect," *IEEE Trans. Mag.,* vol. 49, pp. 1327-1333, 2013.

[5] S. M. Gillette, A. L. Geiler, D. Gray, D. Viehland, C. Vittoria and V. G Harris, "Improved Sensitivity and Noise in Magneto-Electric Magnetic Field Sensors by Use of Modulated AC Magnetostriction," *IEEE Mag. Lett.,* vol. 2, p. 2500104, 2011.

[6] A. Pantinakis and D. A. Jackson, "limitations of an amorphousmetal magnetometer operated by modulating the magnetostrictive strain," *J. Appl. Phys.,* vol. 65, p. 2872, 1989.

[7] X. Zhuang, M. Lam Chok Sing, C. Dolabdjian, Y. Wang, P. Finkel and D. Viehland, "Sensitivity and Noise Evaluation of a Bonded Magneto(elasto)Electric Laminated Sensor Based on In-plane Magneto-capacitance Effect for Quasi-static Magnetic Field Sensing," *IEEE Trans. Mag.,* vol. 51, p. 1, 2015.

[8] M. I. Bichurin and V. M. Petrov, "Modeling of magnetoelectric interaction in magnetostrictive-Piezoelectric Composites," *Adv. Cond. Matter Phys.,* vol. 2012, 2012.

[9] M. I. Bichurin, V. M. Petrov and G. Srinivasan, "Theory of low-frequency magnetoelectric coupling in magnetostrictive-piezoelectric bilayers," *Phys. Rev. B,* vol. 68, p. 054402, 2003.

[10] S. Dong, J.-F. Li and D. Viehland, "Longitudinal and Transverse Magnetoelectric Voltage Coefficients of Magnetostrictive/Piezoelectric Laminate Composite:Experiments," *IEEE Trans. on ultrasonics Ferr. and Freq. Control,* vol. 51, p. 79, 2004.

[11] F. Yang, Y. M. Wen, P. Li, M. Zheng and L. X. Bian, "Resonant magnetoelectric response of magnetostrictive/piezoelectric laminate composite in consideration of losses," *Sensor Actua. A Phys.,* vol. 141, p. 129, 2008.

[12] P. Mohanty, D. A. Harrington, K. L. Ekinci, Y. T. Yang, M. J. Murphy and M. L. Roukes, "Intrinsic dissipation in high-freqeuncy micromechanical resonators," *Phys. Rev. B,* vol. 66, p. 085416, 2002.

[13] A. Grib, D. Heinert, R. Nawrodt, C. Schwarz, V. Grobe, P. Seidel, I. Martin, S. Rowan and J. Hough, "Acoustic losses in a thick quartz plate at low temperatures," *J. Appl. Phys.,* vol. 107, p. 013504, 2010.

[14] M. Brissaud, «Matériaux piézoélectriques,» *Presses polytechniques et*

universitaires Romandes, 2007.

[15] Z. Xing, S. Dong, J. Zhai, L. Yan, J. Li and D. Viehland, "Resonant bending mode of Terfenol-D/steel/Pb(Zr,Ti)O3 magnetoelectric laminate composites," *Appl. Phys. Lett.,* vol. 89, p. 112911, 2006.

[16] J. Gao, Y. Shen, Y. Wang, P. Finkel, J. Li and D. Viehland, "Magnetoelectric Bending-Mode Structure Based on Metglas/Pb(Zr,Ti)O3 Fiber Laminates," *IEEE Trans. on Ultrasonics, Ferr., and Freq. Control,* vol. 58, pp. 1545-1549, 2011.

[17] X. Zhuang, M. Lam Chok Sing, C. Cordier, S. Saez, C. Dolabdjian, J. Das, J. Gao, J. Li and D. Viehland, "Analysis of Noise in Magnetoelectric Thin-Layer Composites Used as Magnetic Sensors," *IEEE Sensor J.,* vol. 11, p. 2183, 2011.

[18] C. A. Grimes, S. C. Roy, S. Rani and Q. Cai, "Theory, Instrumentation and Applications of Magnetoelastic Resonance Sensors: A Review," *Sensors,* vol. 11(3), pp. 2809-2844, 2011.

[19] T. Huber, B. Bergmair, C. Vogler, F. Bruckner, G. Hrkac and D. Suess, "Magnetoelastic resonance sensor for remote strain measurements," *Appl. Phys. Lett.,* vol. 101, p. 042402, 2012.

[20] J. Petrie, D. Viehland, D. Gray, S. Mandal, G. Sreenivasulu, G. Srinivasan and A. S. Edelstein, "Enhancing the sensitivity of magnetoelectric sensors by increasing the operating frequency," *J. Appl. Phys.,* vol. 110, p. 124506, 2011.

[21] Y. Yao, Y. Hou, s. Dong, X. Huang, Q. Yu and X. Li, "Influence of magnetic fields on the mechanical loss of Terfenol-D/$PbZr_{0.52}Ti_{0.48}O_3$/Terfenol-D laminated composites," *J. Alloy Comp.,* vol. 509, p. 6920, 2011.

[22] Y. N. Huang, Y. N. Wang and H. M. Shen, "Internal friction and dielectric loss related to domain walls," *Phys. Rev. B,* vol. 46, pp. 3290-3295, 1992.

[23] H. T. Hardner, M. B. Weissman, M. B. Salamon and S. S. P. Parkin, "Fluctuation-dissipation relation for giant magnetoresistance 1/f nosie," *Phys. Rev. B,* vol. 48, p. 16156, 1993.

[24] Y. Zhuang, S. O. Ural, A. Rajapurkar, S. Tuncdemir, A. Amin and K. Uchino, "Derivation of Piezoelectric Losses from Admittance Spectra," *J. J. Appl. Phys.,* vol. 48, p. 041401, 2009.

[25] J. Hu, W. Tian, J. Zhao, M. Pan, D. Chen and G. Tian, "Remedying magnetic hysteresis and 1/f noise for magnetoresistive sensors," *Appl. Phys. Lett.,* vol. 102, p. 054104, 2013.

[26] S. Zhang, F. Li, J. Luo, R. Xia, W. Hackenberger and T. R. Shrout, "Investigation of single and multidomain $Pb(In_{0.5}Nb_{0.5})O_3$–$Pb(Mg_{1/3}Nb_{2/3})O_3$–$PbTiO_3$ crystals with mm2 symmetry," *Appl. Phys. Lett.,* vol. 97, p. 132903, 2010.

[27] T. M. Correia, J. S. Young, R. W. Whatmore, J. F. Scott, N. D. Mathur and Q. Zhang, "Investigation of the electrocaloric effect in a $PbMg_{2/3}Nb_{1/3}O_3$-$PbTiO_3$ relaxor thin film," *Appl. Phys. Lett. ,* vol. 95, p. 182904, 2009.

[28] F. A. Levinzon, "Noise of Piezoelectric Accelerometer With Integral FET Amplifier," *IEEE Sensor J. ,* vol. 5, p. 1235, 2005.

[29] X. Zhuang, M. Lam Chok Sing, C. Dolabdjian, Y. Wang, P. Finkel, J. Li, and D. Viehland, "Mechanical noise limit of a strain coupled magneto(elasto)electric sensor operating under a magnetic or an electric field modulation," *IEEE Sensor J.,* vol. 15, pp. 1575-1587, 2015.

[30] A. N. Cleland, "Thermomechanical noise limits on parametric sensing with nanomechanical resonators," *New J. Phys.,* vol. 7, p. 235, 2005.